

---

# Visualization Data Analysis

**Tobin Munsat**

*University of Colorado*

*Center for Integrated Plasma Studies*

**US-KSTAR Workshop**

**San Diego, CA**

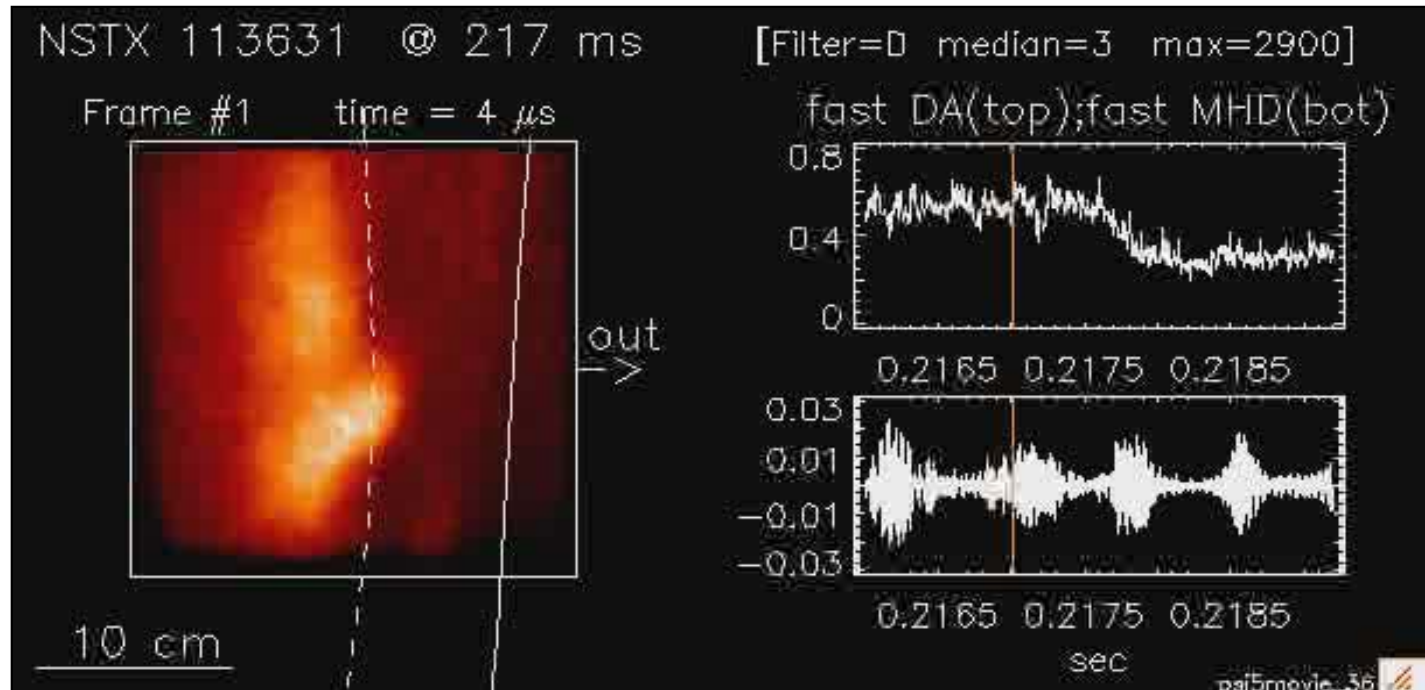
**April 15, 2009**

# Intro

- KSTAR will have a suite of imaging diagnostics very early on (SXR, BES, ECEI/MIR, etc.)
- Data is very dense and rich!
- Analysis methods can be developed and shared between measurements
  
- *Information in basic graphical images*
- *Correlation and coherency*
- *Frequency/wavenumber visualization*
- *Bispectral analysis*
- *Velocimetry*

# Qualitative information from graphical image sets

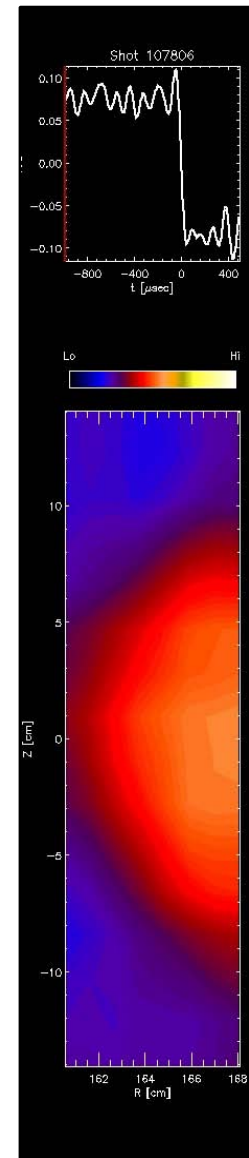
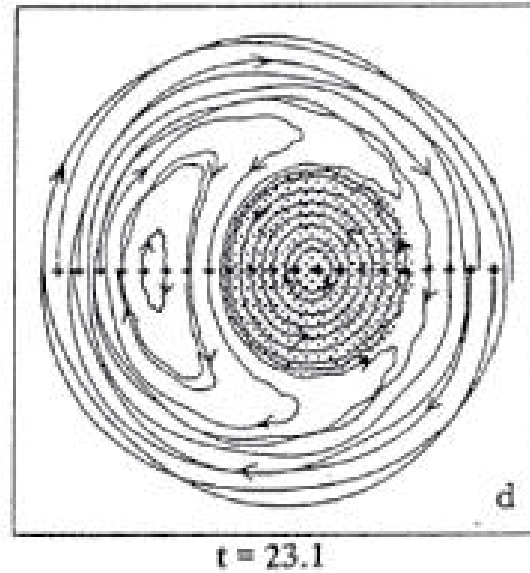
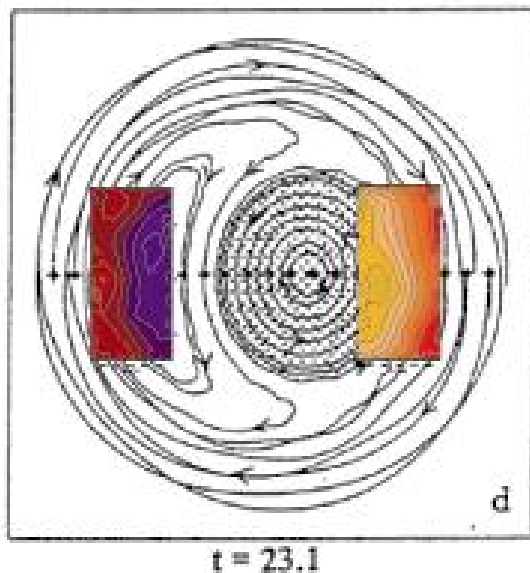
- NSTX shot 113631 (GPI movie)
- Highly intermittent transport
- 2-D view of  $\tilde{n}_e$  at H-mode transition



# Qualitative information from graphical image sets

## *ECEI comparison with topology from MHD models of sawtooth crashes*

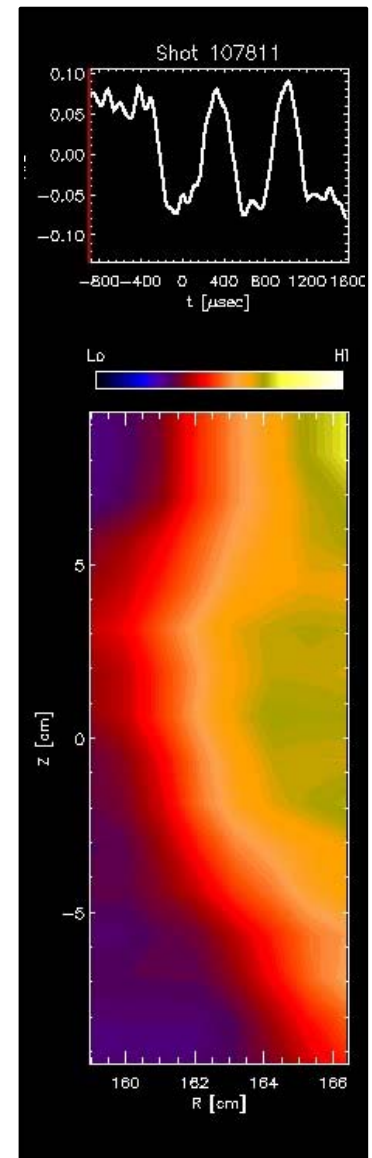
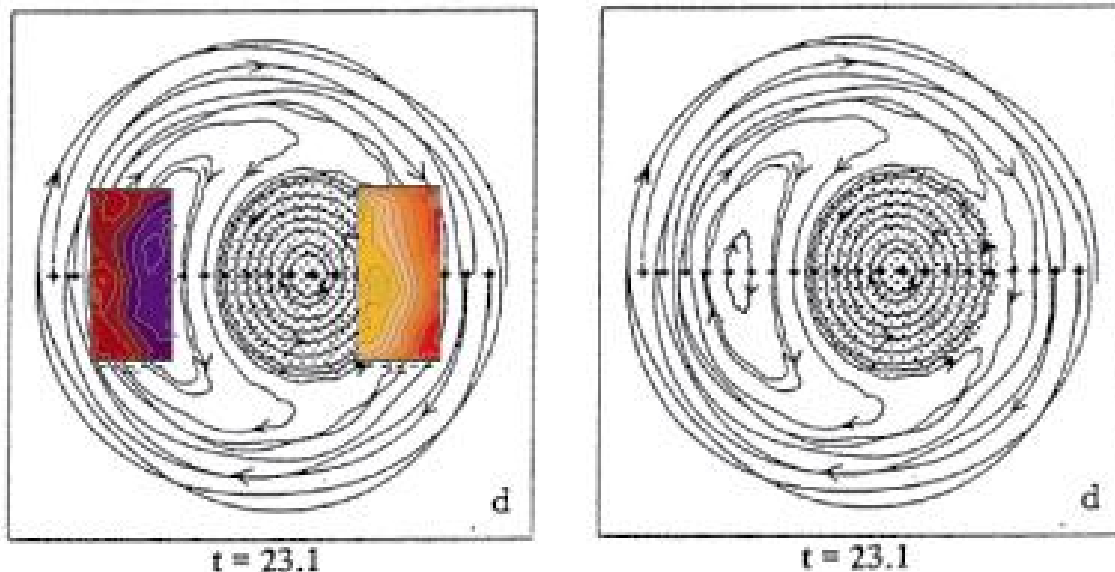
- Resemblance between 2-D images of the hot spot/island and images from simulation results of the full reconnection model (tearing type) (Sykes et al.)
- High-field side crashed clearly observed
- Partial sawtooth observed/characterized
- Projection of 2-D images determines poloidal and toroidal localization/extent of reconnection zone



# Qualitative information from graphical image sets

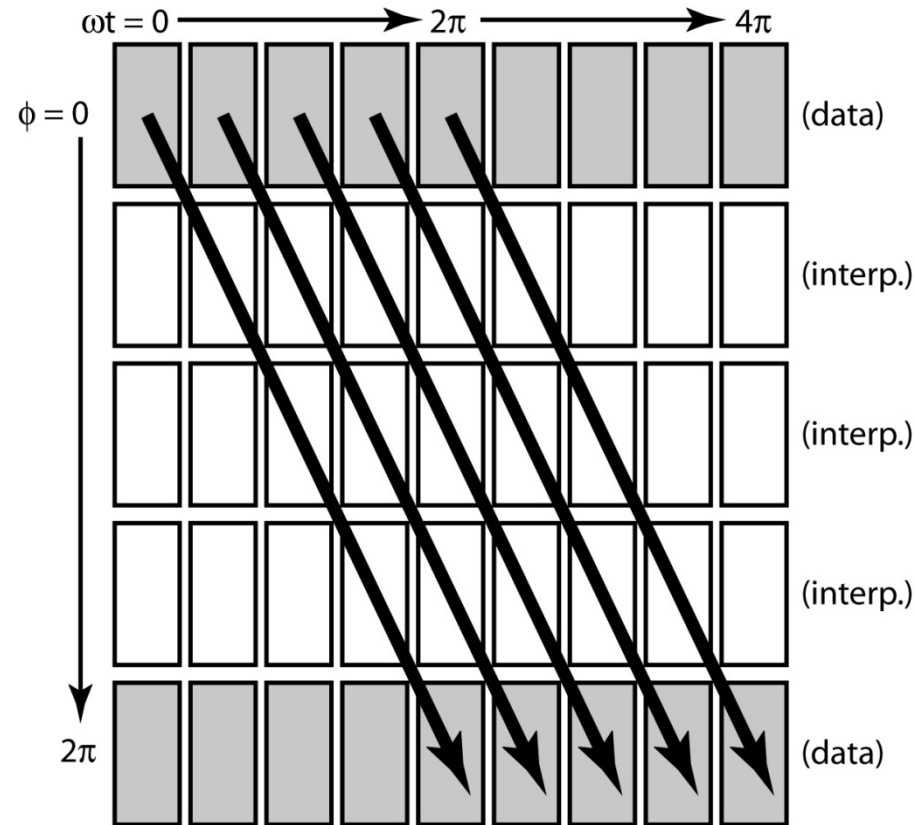
## *ECEI comparison with topology from MHD models of sawtooth crashes*

- Resemblance between 2-D images of the hot spot/island and images from simulation results of the full reconnection model (tearing type) (Sykes et al.)
- High-field side crashed clearly observed
- Partial sawtooth observed/characterized
- Projection of 2-D images determines poloidal and toroidal localization/extent of reconnection zone



# 3-d projection from toroidally spaced systems

- Poloidal view of  $q=1$  surface directly observed in *lab frame*
- *Plasma frame* views can be extracted by interpolation (toroidally rotating plasma where  $\tau_{\text{evolution}} \gg \tau_{\text{rotation}}$ )
- Quantify poloidal extent and time history of image moving through view
- Toroidal extent of particular  $q=1$  helical arc estimated by exclusion from view
- *Toroidal information can be directly quantified with multiple toroidal views*



Vertical: fixed  $t$ , resolved in  $\phi$

Horizontal: fixed  $\phi$ , resolved in  $t$

Diagonal: fixed  $\phi$  in *lab frame*

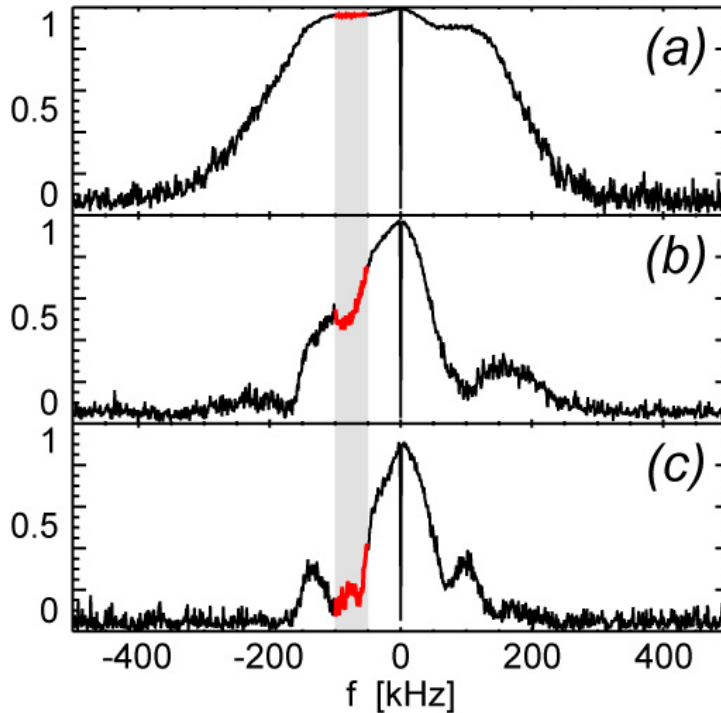
# Cross spectra and coherency

Cross-coherency calculated between poloidally separated channels

$$\gamma_{xy}^2(f) = \frac{|G_{xy}(f)|^2}{G_{xx}(f) \cdot G_{yy}(f)}$$

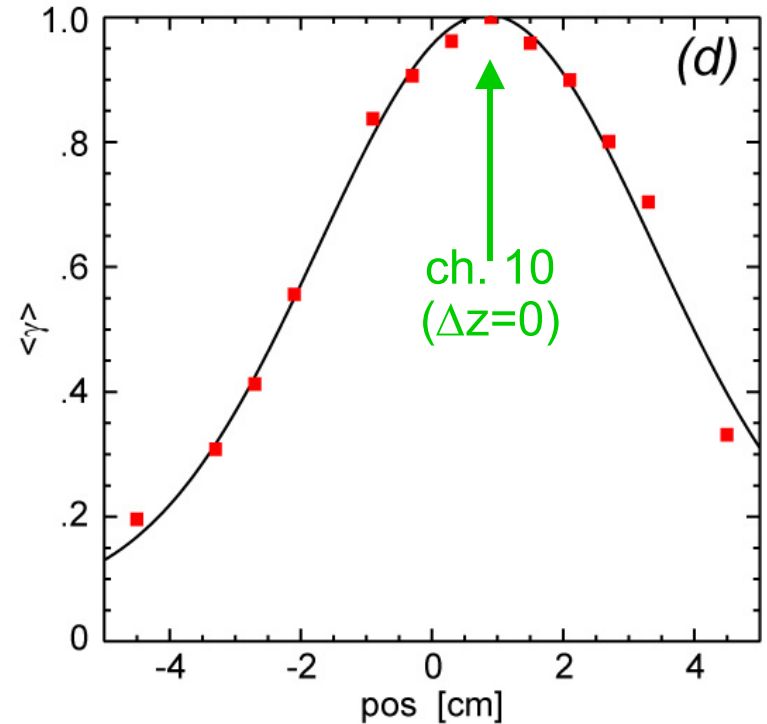
$$G_{xy}(f) = \frac{2}{T} (X^*(f) \cdot Y(f))$$

ch. 10 & 9  
 $\Delta z = 0.6$  cm



ch. 10 & 5  
 $\Delta z = 3.0$  cm

ch. 10 & 1  
 $\Delta z = 5.4$  cm

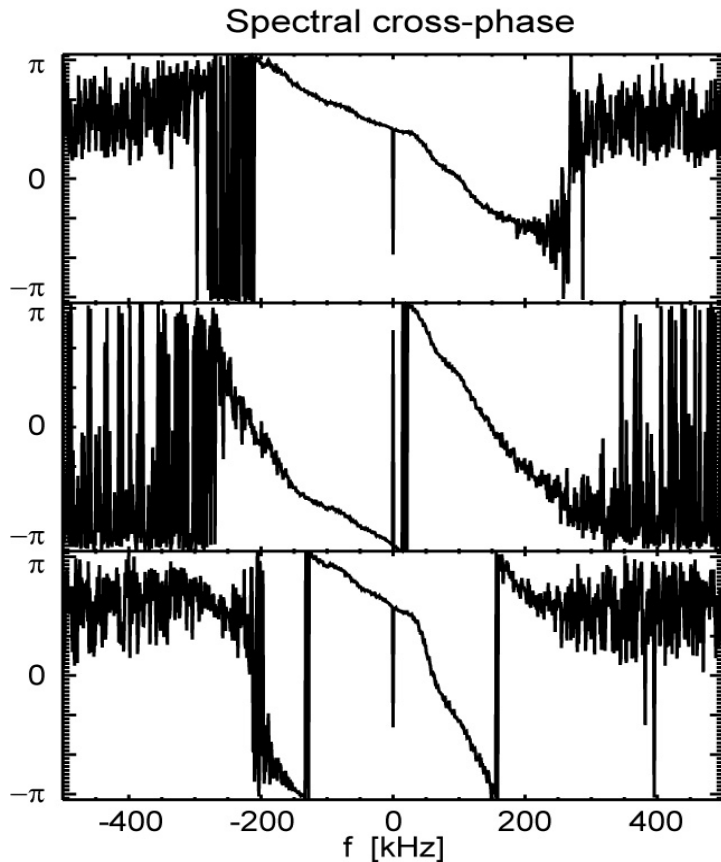


# Cross spectra and coherency

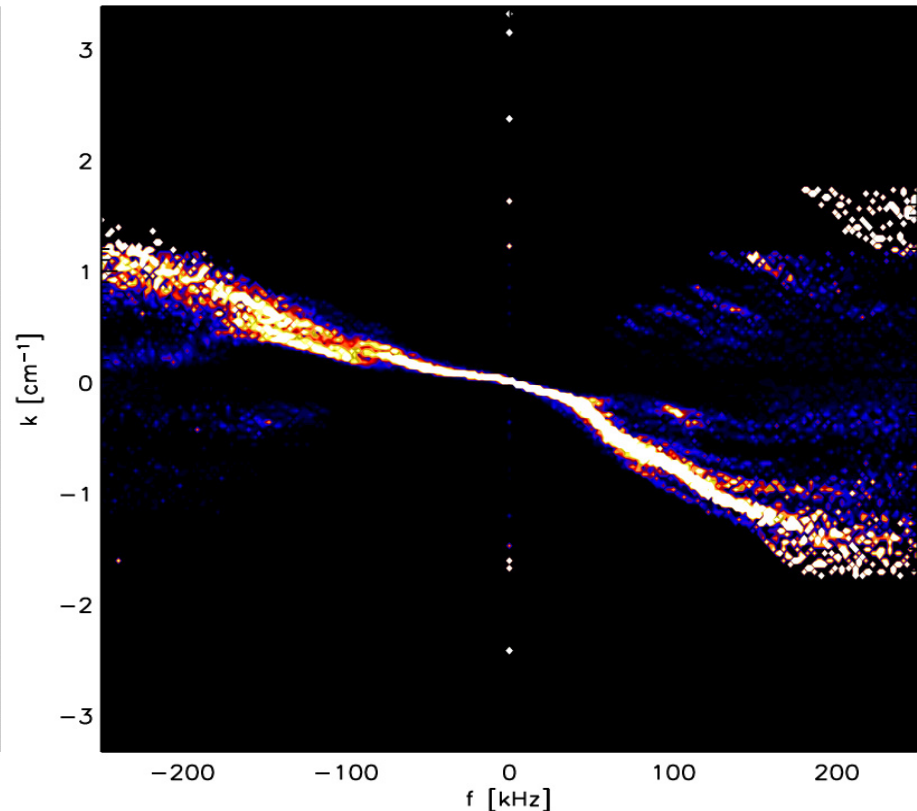
Cross-phase for all channel pairs  
(weighted cross-spectral power)  
combined into map of cross-power vs. f,k

$$\phi(f) = \tan^{-1} \left[ \frac{\text{im}(G_{xy})}{\text{re}(G_{xy})} \right]$$

$$k(f) = \frac{\phi(f)}{\Delta Z}$$



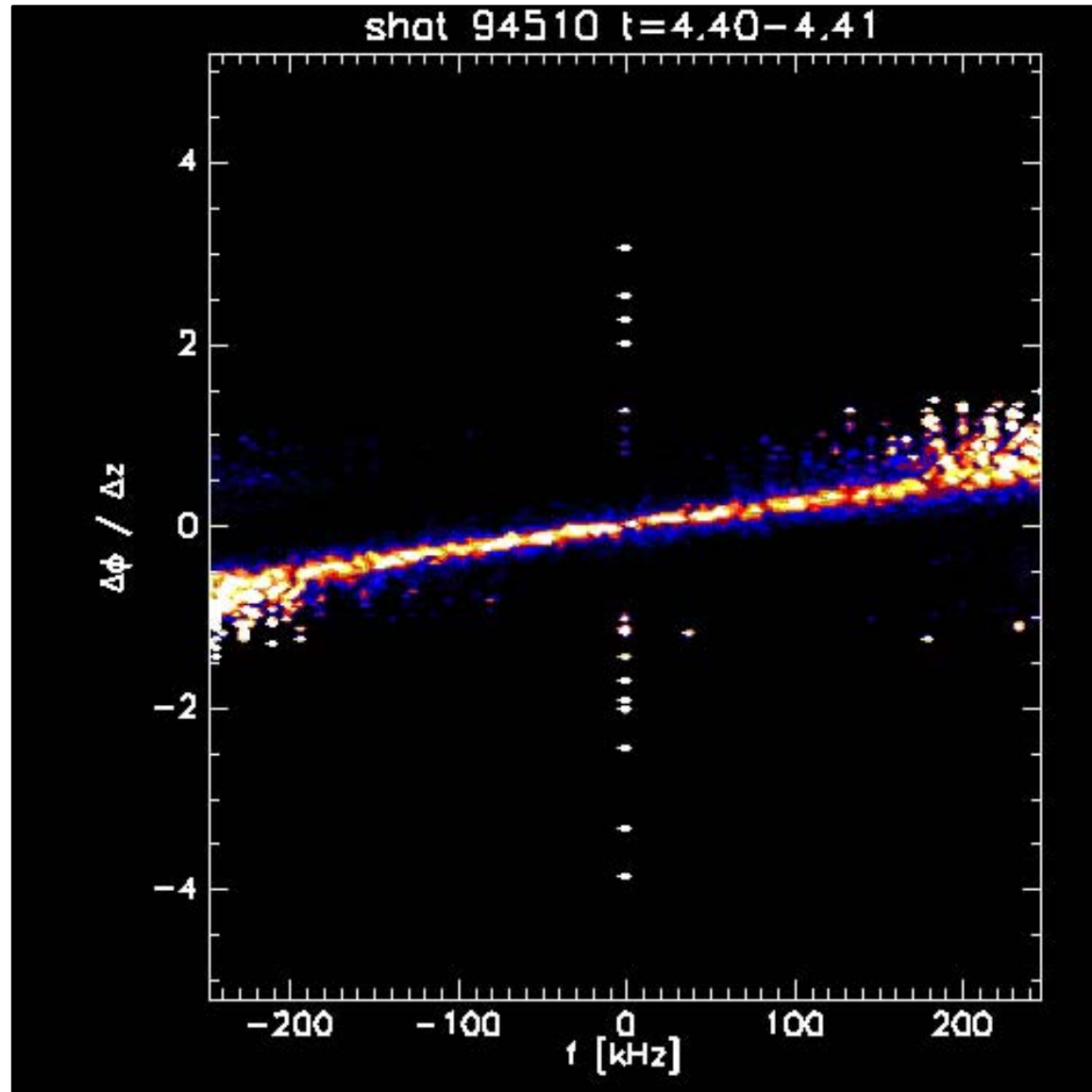
k vs. f for shot 94180 t=1.00–1.50



# Cross spectra and coherency

Co-injected beam spins up plasma, then rotation reverts to electron-diamagnetic direction after NBI turn-off.

More complicated 'dispersion relations' can emerge from coherency analysis of imaged data



# Bispectral Analysis

Measure of *coherence* between waves satisfying coupling/resonance conditions:  $\omega_1 + \omega_2 = \omega_3$   $k_1 + k_2 = k_3$   
(To discern *coupled* waves from independent modes)

## Bispectrum

$$B = \langle Z_1 Z_2 Z_3^* \rangle$$

## Bicoherence

$$b = \sqrt{\frac{|B|^2}{\langle |Z_1 Z_2|^2 \rangle \langle |Z_3|^2 \rangle}}$$

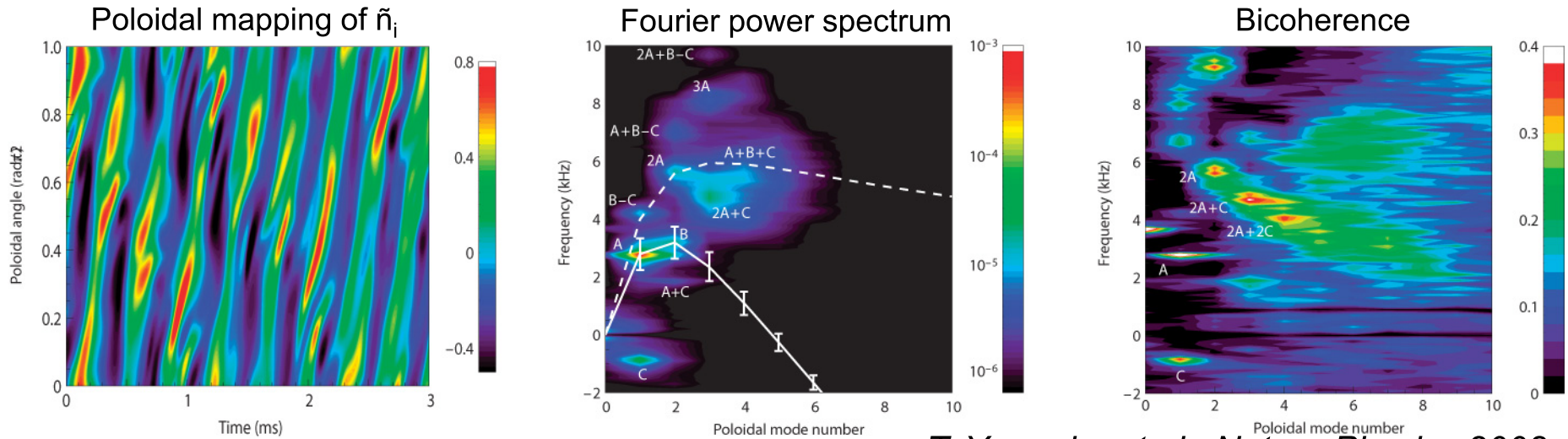
## Biphase

$$\varphi_b = \tan^{-1} \frac{\text{Im}(b)}{\text{Re}(b)}$$

- *Spectral power transfer in plasma turbulence*
- *Turbulent energy cascading*
- *Nonlinear waves/structures from self-excited fluctuations*

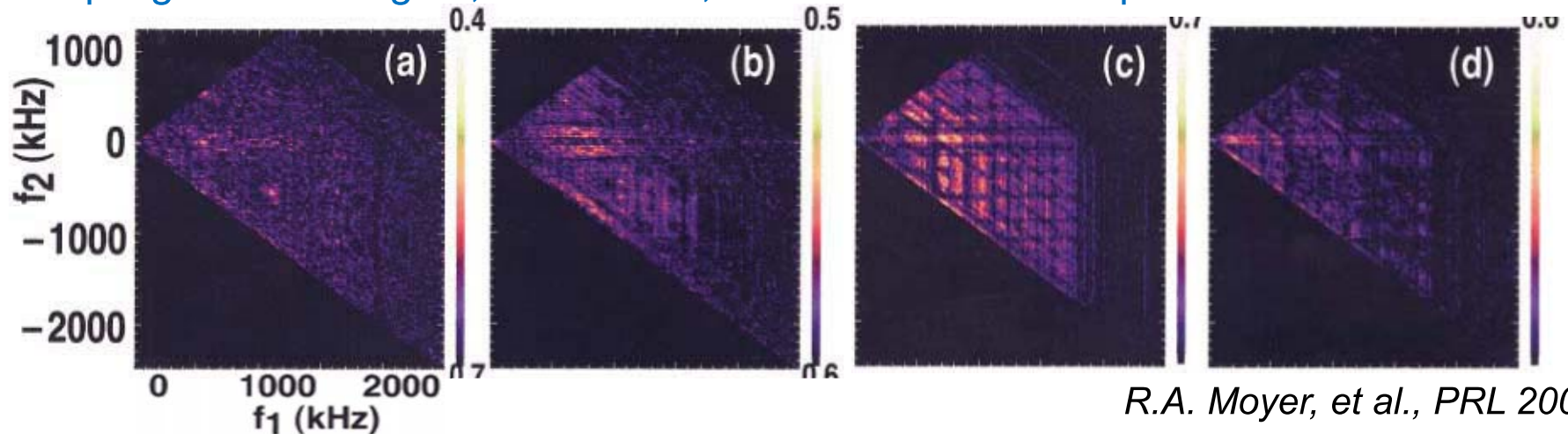
# Bispectral Analysis

Coupling of drift waves & flute mode  $\rightarrow$  cascade to smaller-scale fluctuations:



*T. Yamada, et al., Nature Physics 2008*

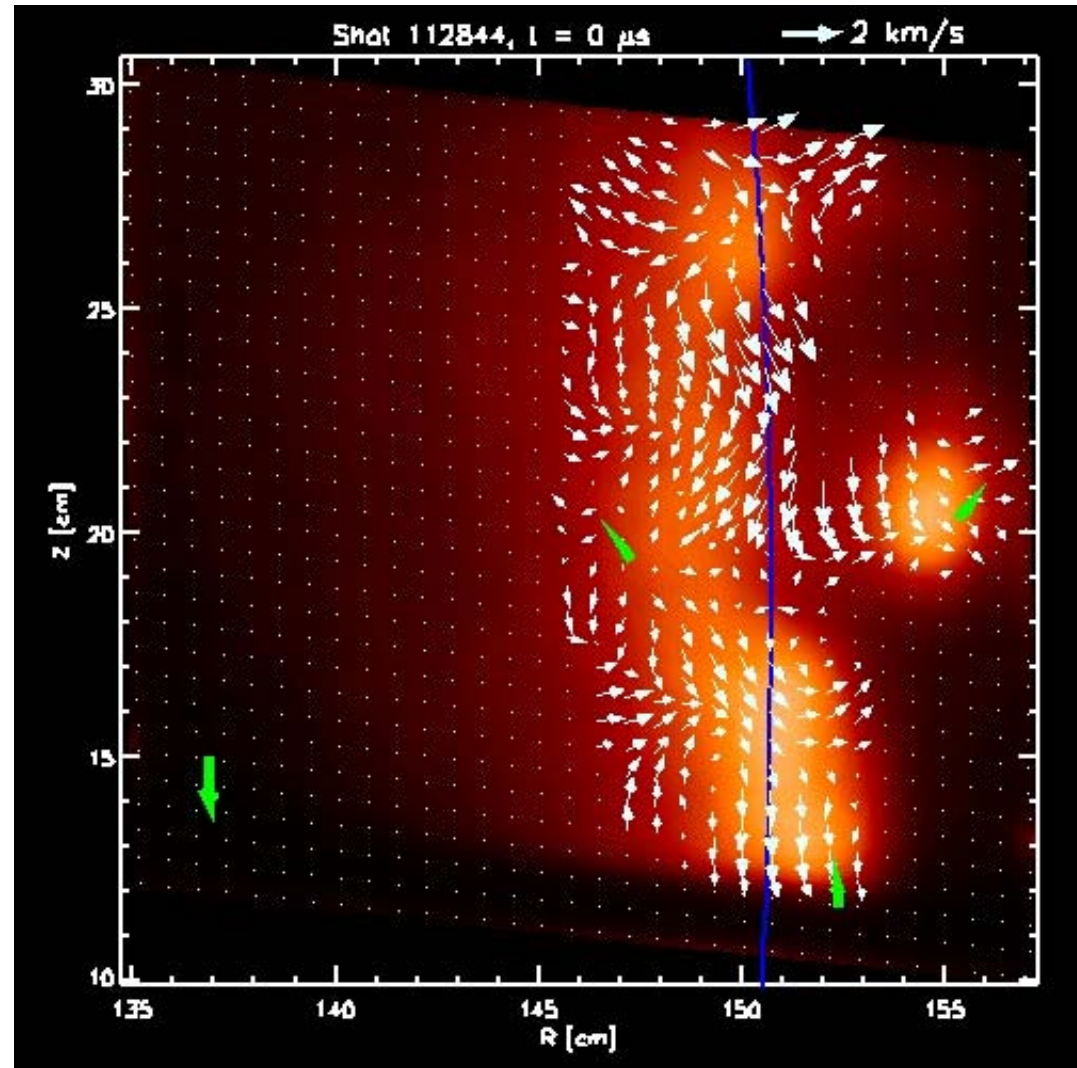
Coupling between high  $k_\omega$  and low  $k_\omega$  fluctuations near separatrix in L-H transition:



*R.A. Moyer, et al., PRL 2001*

# Velocimetry

- Combination of Optical Flow and Pattern Matching techniques used to derive velocity fields from image frames
- Match structure evolution, trajectories, etc. to evolving models
- Characterize turbulent plasmas and assess intermittent transport
- Derive higher-order statistics from dense flow fields



# Optical Flow : The Basics

- Optical flow condition = local constant brightness  
(Solve continuity equation for intensity):

$$\frac{\partial I}{\partial t} + u \frac{\partial I}{\partial x} + v \frac{\partial I}{\partial y} = \frac{\partial I}{\partial t} + \vec{v} \cdot \vec{\nabla} I = 0 \quad \text{where} \quad \vec{v} \equiv (u, v)$$

Now, can define spatial basis functions  $\phi(x, y)$  so that

$$u = \sum_k u_k \phi_k \quad \text{and} \quad v = \sum_k v_k \phi_k$$

$$\frac{\partial I}{\partial t} + \sum_k u_k \phi_k \frac{\partial I}{\partial x} + \sum_k v_k \phi_k \frac{\partial I}{\partial y} = 0$$

(solved for each pixel)

# Optical Flow : Implemented

$$\frac{\partial I}{\partial t} + \sum_k u_k \phi_k \frac{\partial I}{\partial x} + \sum_k v_k \phi_k \frac{\partial I}{\partial y} = 0$$

$$[x_0, x_1, x_2, x_3, x_4, x_5, \dots] \equiv [u_0, v_0, u_1, v_1, u_2, v_2, \dots]$$

$$A_{p,0} \equiv \phi_0 \left[ \frac{\partial I}{\partial x} \right]_p, A_{p,1} \equiv \phi_0 \left[ \frac{\partial I}{\partial y} \right]_p, A_{p,2} \equiv \phi_1 \left[ \frac{\partial I}{\partial x} \right]_p, A_{p,3} \equiv \phi_1 \left[ \frac{\partial I}{\partial y} \right]_p, \dots$$

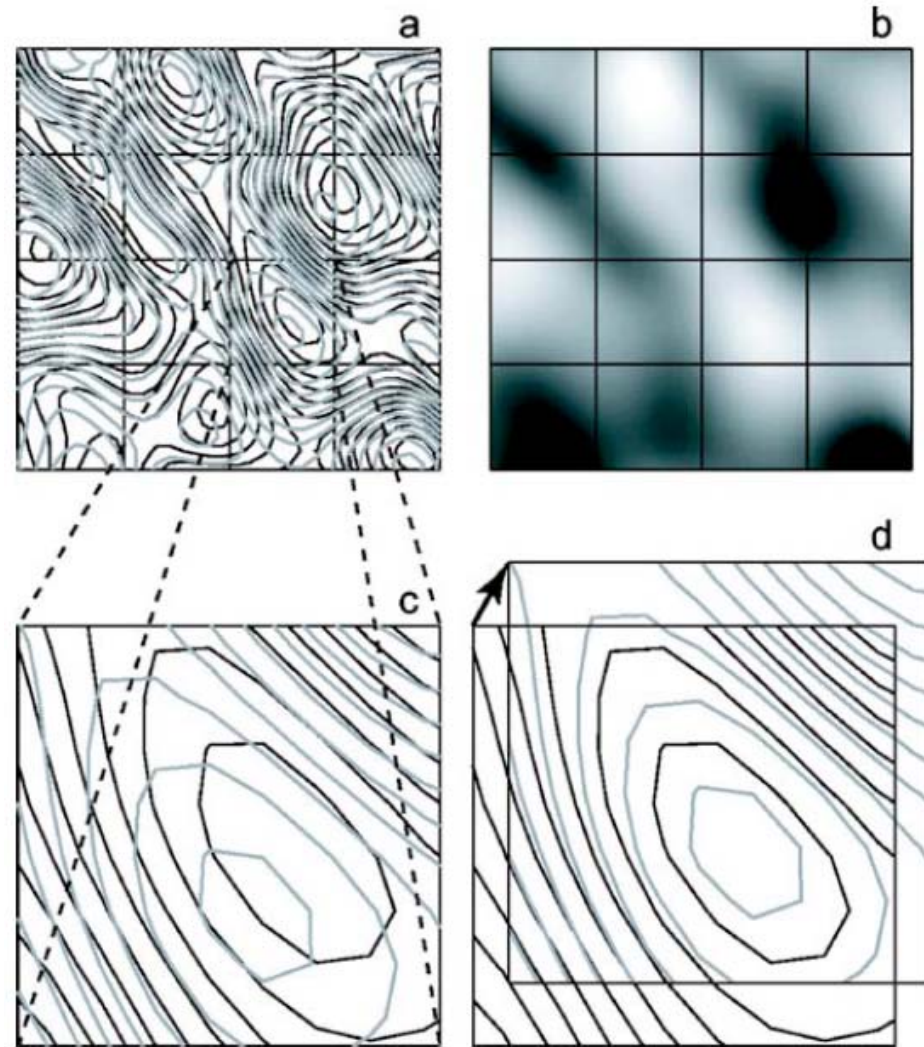
$$B_p \equiv - \left[ \frac{\partial I}{\partial t} \right]_p$$



$$Ax = B$$

# Combined Optical Flow / Pattern Matching

- Decompose each image into grid of tiled sub-images.
- Best matching position is found using error function:
  - Reward smaller integrated absolute difference over each sub-image.
  - Reward (weakly) “smoother” velocity fields. Assumes minimal shearing in true field.
- Velocity field is not constrained to lie along the gradient of the intensity.
- Does not exhibit a maximum velocity limit due to time resolution.
- Output highly dependent on initial guess for velocity field on each frame (use of optical flow output solves this).



# Divergence-Controlled Optical Flow

- Decompose the velocity field into the gradient of *two* scalar potentials:
 
$$\vec{v} = \vec{\nabla} \psi + \vec{\nabla} \phi$$
- Laminar and curl-free flows are captured by the gradient of  $\psi$ , solenoidal flows are captured by the gradient of  $\phi$ 

$$\vec{\nabla} \psi = \vec{v}_{laminar} + \vec{v}_{curl-free}, \quad \vec{\nabla} \times (\vec{\nabla} \psi) = 0$$

$$\vec{\nabla} \phi = \vec{v}_{solenoidal}, \quad \vec{\nabla} \cdot (\vec{\nabla} \phi) = 0$$
- Design minimization functions for each velocity potential that are minimized by the “best” optical flow field estimate with vanishing divergence:

-> Optical flow objective functional

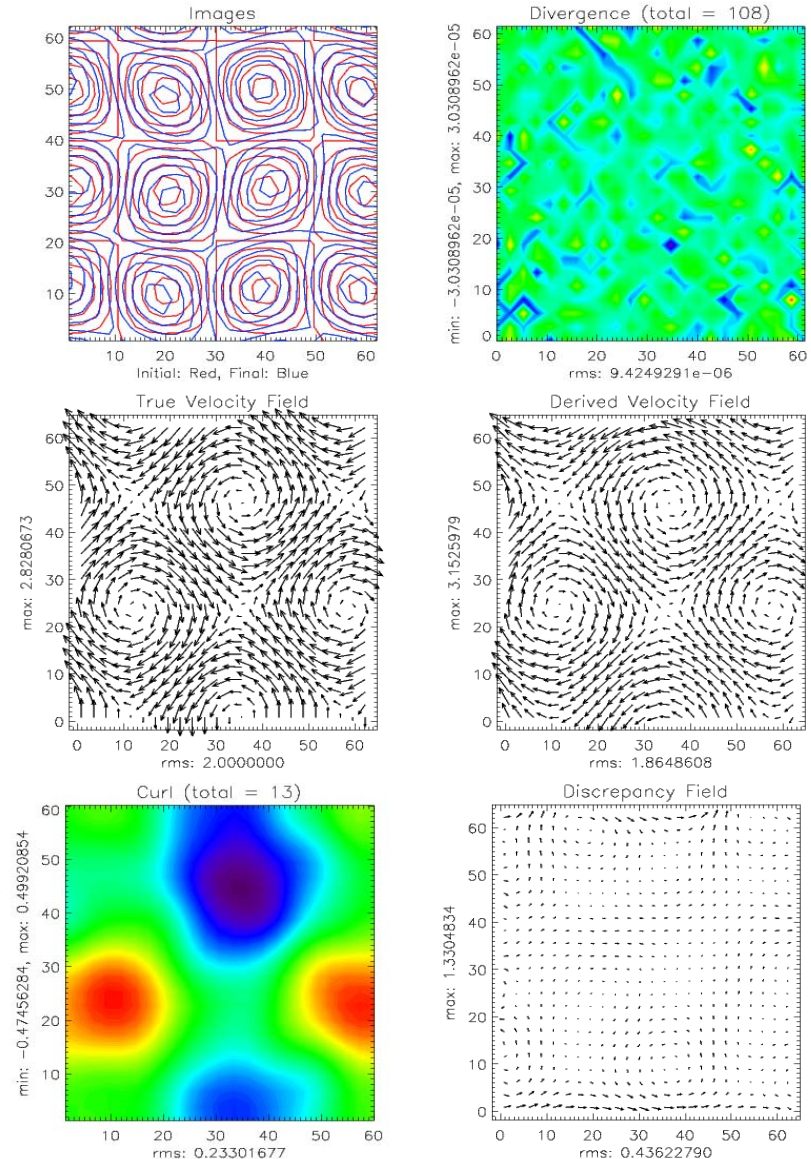
$$J_0(\psi, \phi) = \left| D_t I + \vec{\nabla} I \cdot (\vec{\nabla} \psi + \vec{\nabla} \phi) \right|^2$$

->  $\psi$  Augmented Lagrangian (with  $\phi$  held constant and Lagrange multipliers  $q$ )

$$L_\psi(\psi, \bar{\phi}, q) = J_0(\psi, \bar{\phi}) + \langle q, \vec{\nabla} \cdot (\vec{\nabla} \psi) \rangle + \frac{r}{2} \left| \vec{\nabla} \cdot (\vec{\nabla} \psi) \right|^2 + \frac{\gamma}{2} \left| B_n \cdot \vec{\nabla} \psi \right|^2$$

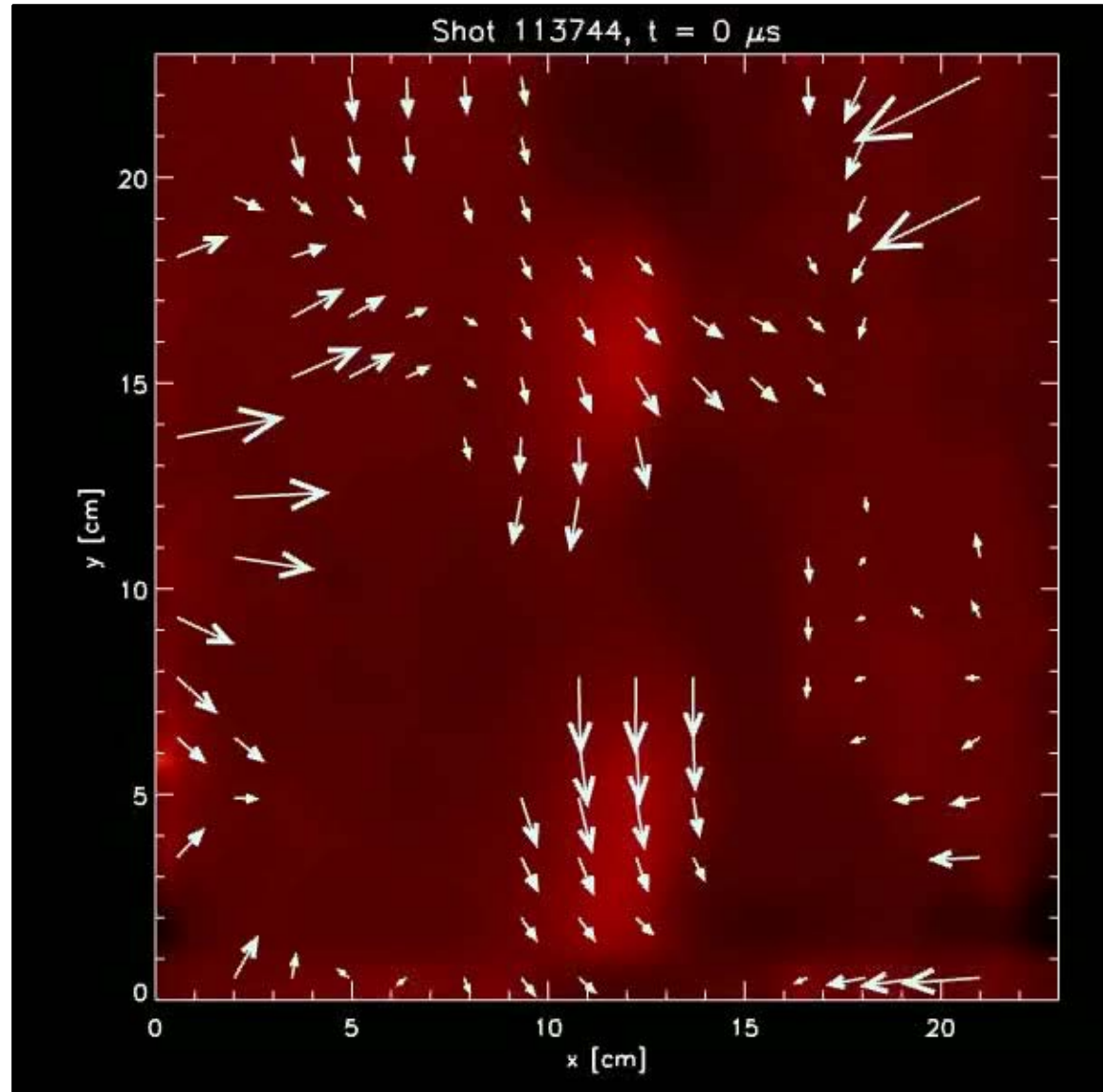
->  $\phi$  objective functional (with  $\psi$  held constant)

$$J_\phi(\bar{\psi}, \phi) = J_0(\bar{\psi}, \phi) + \frac{\lambda_c}{2} \left| \vec{\nabla} (\vec{\nabla} \times (\vec{\nabla} \phi)) \right|^2$$



# Velocimetry on GPI (NSTX)

- “Dense” flow fields
- No a-priori knowledge of velocity behavior required
- No a-priori knowledge of structures required
- Analysis of turbulent flowfields possible
- Techniques applicable to many diagnostic systems



# Concluding remarks

---

- Each technique here can be adapted to many multichannel / imaging instruments
- Techniques have different strengths and weaknesses depending on spatial / time resolution and coverage
- Many crossover studies will be possible!